ENVIRONMENTAL SCIENCE

Terrestrial discharges mediate trophic shifts and enhance methylmercury accumulation in estuarine biota

Sofi Jonsson,[1,2]* Agneta Andersson,[2,3] Mats B. Nilsson,[4] Ulf Skyllberg,[4] Erik Lundberg,[2] Jeffra K. Schaefer,[5] Staffan Åkerblom,[6] Erik Björn[1†]

2017 © The Authors, some rights reserved; exclusive licensee American Association for the Advancement of Science. Distributed under a Creative Commons Attribution NonCommercial License 4.0 (CC BY-NC).

The input of mercury (Hg) to ecosystems is estimated to have increased two- to fivefold during the industrial era, and Hg accumulates in aquatic biota as neurotoxic methylmercury (MeHg). Escalating anthropogenic land use and climate change are expected to alter the input rates of terrestrial natural organic matter (NOM) and nutrients to aquatic ecosystems. For example, climate change has been projected to induce 10 to 50% runoff increases for large coastal regions globally. A major knowledge gap is the potential effects on MeHg exposure to biota following these ecosystem changes. We monitored the fate of five enriched Hg isotope tracers added to mesocosm scale estuarine model ecosystems subjected to varying loading rates of nutrients and terrestrial NOM. We demonstrate that increased terrestrial NOM input to the pelagic zone can enhance the MeHg bioaccumulation factor in zooplankton by a factor of 2 to 7 by inducing a shift in the pelagic food web from autotrophic to heterotrophic. The terrestrial NOM input also enhanced the retention of MeHg in the water column by up to a factor of 2, resulting in further increased MeHg exposure to pelagic biota. Using mercury mass balance calculations, we predict that MeHg concentration in zooplankton can increase by a factor of 3 to 6 in coastal areas following scenarios with 15 to 30% increased terrestrial runoff. The results demonstrate the importance of incorporating the impact of climate-induced changes in food web structure on MeHg bioaccumulation in future biogeochemical cycling models and risk assessments of Hg.

INTRODUCTION

Mercury is considered one of the top 10 chemicals of public health concern by the World Health Organization (www.who.int) and is the most common reason for human health–related fish consumption advisories by the U.S. Environmental Protection Agency (http://water.epa.gov/). Future risks of Hg in the environment depends on the success of reducing Hg emissions and the impact of ecosystem processes on the reactivity and mobility of legacy Hg accumulated in sediment, soil, and water (*1*–*3*). As described in the following text, a major knowledge gap exists regarding how altered loading rates of terrestrial natural organic matter (NOM) and nutrients may control MeHg net formation and bioaccumulation in coastal ecosystems by modulating the productivity and structure of the pelagic food web.

Marine ecosystems, and mainly their coastal zones, have been estimated to contribute more than 60% of the total economic value of the biosphere (*4*). These ecosystem services are currently threatened by anthropogenic pollution and a changing climate. Increased terrestrial water runoff and accompanied input of terrestrial NOM and nutrients to lakes and coastal sea areas have been observed in several regions during the late 20th century (*5*–*8*). These increases are predicted to escalate for large regions worldwide following increased air temperatures and precipitation events (*7*). Methylmercury in estuarine systems originates from direct terrestrial and atmospheric MeHg inputs and from in situ formation in the water column and in sediment (*9*). The degree of bioaccumulation can differ for these MeHg pools that, together with their size, control their contribution to MeHg concentrations in estuarine biota (*10*). It has been suggested that increased input of terrestrial NOM to coastal ecosystems may increase total Hg loading to the systems (*11*) and MeHg formation in the water column (*12*). In addition, increased terrestrial NOM concentration in water decreases light penetration and, accordingly, photosynthetic primary production and could potentially fuel the pelagic bacterial food web (*6*, *13*). This may result in a shift in basal resource of the food web, from autotrophic to heterotrophic, and decreased sedimentation of autochthonous NOM (*14*). An autotrophic food web is defined by photosynthetic primary production exceeding the heterotrophic bacterial production, whereas in a heterotrophic food web, the heterotrophic bacterial production exceeds the photosynthetic primary production. In contrast to terrestrial NOM loadings, eutrophication caused by N and P input may lead to higher abundances of plankton and thus increased sedimentation rates of autochthonous NOM (*14*). It has been shown that benthic anaerobic bacteria primarily use metabolic electron donors originating from autochthonous NOM (rather than allochthonous NOM) (*15*, *16*). Further, high MeHg formation rates in estuarine sediment have been related to low C/N molar ratio (*17*, *18*), suggesting also that the activity of bacteria with the capacity of methylating inorganic divalent Hg (Hg^{II}) to MeHg (*19*, *20*) could be driven by autochthonous NOM. The increased input of terrestrial NOM could therefore hypothetically lead to a decreased MeHg formation rate. The type and the amount of NOM occurring in the pelagic zone also influence the chemical speciation of MeHg and thus its availability for bioaccumulation at the lowest level of the food web, as demonstrated for freshwater (*21*, *22*) and marine (*23*) plankton species. Pelagic NOM may also indirectly control the biomagnification efficiency of

[1]Department of Chemistry, Umeå University, SE-901 87 Umeå, Sweden. [2]Umeå Marine Sciences Centre, Umeå University, SE-910 20 Hörnefors, Sweden. [3]Department of Ecology and Environmental Science, Umeå University, SE-901 87 Umeå, Sweden. [4]Department of Forest Ecology and Management, Swedish University of Agricultural Sciences, SE-901 83 Umeå, Sweden. [5]Department of Environmental Sciences, Rutgers University, New Brunswick, NJ 08901, USA. [6]Department of Aquatic Sciences and Assessment, Swedish University of Agricultural Sciences, SE-750 07 Uppsala, Sweden.
*Present address: Department of Marine Sciences, University of Connecticut, 1080 Shennecossett Road, Groton, CT 06340, USA.
†Corresponding author. Email: erik.bjorn@umu.se

Downloaded from http://advances.sciencemag.org/ on June 27, 2017

MeHg by affecting the planktonic biomass [and thus the biodilution of MeHg (*24*)] and the length of the food web, that is, the number of biomagnification steps (*25*). The overall effect of changes in structure and dynamics of the pelagic food web on MeHg net formation and bioaccumulation is thus complex and challenging to predict (*2*, *3*, *25*).

Here, we test the hypotheses that inorganic nutrient and terrestrial NOM loadings to estuarine ecosystems control (i) MeHg formation in sediment (by controlling the type and the amount of NOM supplied to the benthic zone) and (ii) MeHg bioaccumulation in the pelagic food web (by controlling the structure and productivity of the food web).

RESULTS

Ecological and biogeochemical conditions in the mesocosm model ecosystems

We used a recently developed isotope tracer methodology (*10*, *26*) in an experimental mesocosm setup with brackish water [salinity of 5 practical salinity unit (PSU)] and intact sediment cores [n = 12; 4.9 × 0.73 m (height × diameter), 2000 liters of water, and ≈0.2 × 0.63 m (depth × diameter) sediment core], maintaining natural redox gradients and microorganism community structure. We applied three mesocosm treatment schemes: (i) low nutrient loading, (ii) high nutrient loading, and (iii) low nutrient loading combined with the addition of terrestrial NOM, referred to as NP_{low}, NP_{high}, and TM, respectively (fig. S1 and table S1). The NP_{low} treatment was designed to represent present-day conditions in the brackish water environment of the Bothnian Sea (*27*) off the Swedish east coast. A scenario of increased eutrophication was represented by NP_{high}, and increased terrestrial runoff, for example, following regional climate change scenarios (*28*, *29*), was represented by TM. On the basis of data from the low nutrient addition treatment (NP_{low}), Jonsson *et al.* (*10*) demonstrated the importance of differentiated availability of geochemical Hg pools in sediment, atmospheric deposition, and catchment runoff for MeHg formation and bioaccumulation (part of the data in Table 1 and figs. S2 and S3). Here, we demonstrate how ecosystem changes caused by shifts in food web structure by terrestrial NOM and nutrient loadings control MeHg formation and bioaccumulation.

Autotrophic pelagic systems, with moderate and high photosynthetic primary production, were created by the NP_{low} and NP_{high} treatments, respectively, and a heterotrophic system with low productivity by the TM. The photosynthetic primary production contributed 54 ± 1% (average ± SE), 54 ± 4%, and 28 ± 2% of the total production in the three treatments, respectively (Table 1 and fig. S2). In comparison with the two NP treatments, the TM treatment on average increased the dissolved organic carbon (DOC) concentration from 4.8 ± 0.12 to 5.6 ± 0.10 mg liter^{-1} and the concentration of humic substances from 18 ± 0.3 to 27 ± 0.5 μg liter^{-1} (quinine sulfate units) (Table 1). Although both autochthonous and allochthonous organic carbons contribute to DOC, the humic substances content, as determined by fluorescence spectroscopy, is used as a relative proxy of terrestrial organic matter. The observed increases in water-phase DOC and humic substance content in the TM treatment are in good agreement with regional future climate scenarios, proposing a 15 to 50% increase in terrestrial runoff (*28*, *29*). This corresponds to a predicted increase in DOC of 10 to 40% in the coastal Bothnian Sea given that 75% of the DOC in this region is of terrestrial origin (*30*). The magnitude of the increase in DOC concentration for the TM treatment is also relevant for climate change–induced runoff scenarios for large coastal regions worldwide (fig. S4) (*7*). However, it should be noted that the interpretations of data recently compiled by the Intergovernmental Panel on Climate Change (IPCC) (*7*) project a highly variable response in runoff with altered climate, with either increases or decreases, for different regions globally.

Solid/adsorbed Hg tracers in the form of metacinnabar (β-$^{200}HgS_{sed}$) and Hg^{II} and MeHg bonded to thiol groups in NOM ($^{201}Hg^{II}$-NOM_{sed} and $Me^{198}Hg$-NOM_{sed}) were synthesized and added to the intact sediment to represent accumulated Hg pools. The tracers were injected at 0.5-cm sediment depth, below the redoxcline, where conditions are favorable for MeHg formation. Aqueous Hg^{II} and MeHg tracers ($^{204}Hg^{II}{}_{wt}$ and $Me^{199}Hg_{wt}$) were added as dissolved hydroxyl complexes to the water phase to represent recent Hg inputs from atmospheric deposition and terrestrial runoff (fig. S1) (*10*). As demonstrated by calculations, these tracers are expected to readily form complexes with thiol groups in dissolved NOM (table S2) (*10*). The major fraction of the aqueous tracers successively deposited to the sediment surface during the experiment (fig. S3).

Table 1. Summary table of average (SE) measured pelagic variables and MeHg net formation in the sediment under three different experimental treatments. Average values (SE) (n = 20 to 40) during the 53-day experiment are given for each parameter. Different capital letters (A to C) indicate statistically significant (P < 0.05, repeated-measures ANOVA) differences between treatments, that is, rows, for parameters in footnotes (table S3).

	DOC (mg liter^{-1})	Humic subst.* (μg liter^{-1})	Autotrophic prod.† (μmol C dm^{-2} hour^{-1})	Heterotrophic prod.‡ (μmol C dm^{-2} hour^{-1})	Autotrophic fraction§ (%)	Chl a‖ (mg m^{-3})	MeHg/Hg^{II} molar ratio¶ × 10^{-3}		
							β-$^{200}HgS_{sed}$	$^{201}Hg^{II}$-NOM_{sed}	$^{204}Hg^{II}{}_{wt}$
NP_{low}#	4.8 (0.12)^{A}	18 (0.2)^{A}	2.25 (0.25)^{A}	1.94 (0.08)^{A}	54 (1)^{B}	5.60 (0.60)^{AB}	0.49 (0.05)^{AB}	8.4 (1.2)^{A}	26 (6)^{A}
NP_{high}	4.8 (0.07)^{A}	19 (0.3)^{A}	3.21 (0.57)^{A}	2.88 (0.29)^{B}	54 (4)^{B}	10.6 (2.2)^{B}	0.67 (0.12)^{B}	9.2 (1.2)^{A}	27 (8)^{A}
TM	5.6 (0.10)^{B}	27 (0.5)^{B}	0.97 (0.11)^{B}	2.52 (0.25)^{B}	28 (2)^{A}	2.89 (0.20)^{A}	0.40 (0.03)^{A}	7.7 (0.8)^{A}	45 (10)^{A}

*Humic subst., humic substance concentration as determined by fluorescence spectroscopy calibrated in quinine sulfate units. †Autotrophic prod., autotrophic production rate (photosynthetic primary production rate). ‡Heterotrophic prod., heterotrophic bacteria production rate. §Autotrophic fraction, fraction (%) of autotrophic production of the sum of autotrophic and heterotrophic production. ‖Chl a, chlorophyll a. ¶MeHg/Hg^{II} molar ratio measured in sediment for Hg isotope tracers added as metacinnabar to the sediment (β-$^{200}HgS_{sed}$), organic matter Hg complex to the sediment ($^{201}Hg^{II}$-NOM_{sed}), and dissolved Hg^{II} to the water column ($^{204}Hg^{II}{}_{wt}$). #The data for the NP_{low} treatment was reproduced with permission from Jonsson *et al.* (*10*) and the original data can be found in tables S3 and S4 of the source paper.

Downloaded from http://advances.sciencemag.org/ on June 27, 2017

Net formation of MeHg in sediment

We monitored MeHg net formation [quantified as the MeHg/Hg^{II} molar ratio (*10*)] in water and sediment throughout the 2-month experiment. Overall, the experimental treatment effects on MeHg net formation in sediments were relatively small. The average net methylation of the β-$^{200}HgS_{sed}$ and $^{201}Hg^{II}$-NOM_{sed} tracers injected in the sediment was highest for the NP_{high} treatment, intermediate for the NP_{low} treatment, and lowest for the TM treatment (Table 1 and Fig. 1). Differences were statistically significant [repeated-measures analysis of variance (ANOVA)] for β-$^{200}HgS_{sed}$ [$F(2, 6) = 5.42$, $P = 0.045$] but not for $^{201}Hg^{II}$-NOM_{sed} [$F(2, 6) = 0.25$, $P = 0.79$]. The order of treatment response for the tracers agrees with the proposed hypothesis that Hg^{II} methylation in sediments is supported by the pelagic photosynthetic primary production (stimulated by NP additions) controlling the supply of autochthonous NOM to the benthic zone. For natural estuarine ecosystems, the relative fluxes of autochthonous NOM and labile terrestrial organic matter over longer time are expected to determine which type of NOM is more important in controlling sediment microbial activity and Hg^{II} methylation. The significant differences in photosynthetic primary production between mesocosm treatments [Table 1 and fig. S2; repeated-measures ANOVA, $F(2, 6) = 10.83$, $P = 0.010$] were only partly reflected in the sedimentation rate of autochthonous NOM (fig. S5). A higher sedimentation rate was obtained for NP_{high} compared to NP_{low} (ANOVA, $P = 0.008$), but there was no difference between the NP_{low} and TM treatments. These minor differences in sedimentation rates might have caused nonsignificant differences in the activity of microorganisms methylating Hg^{II} in the sediment across these two treatments.

In line with previous studies (*10*, *26*, *31*), we observed large differences in average MeHg net formation for the different tracers [Table 1 and Fig. 1; repeated-measures ANOVA, $F(1, 25) = 65.01$, $P = 0.007$], which followed the order of their expected availability to Hg^{II} methylation bacteria (β-$^{200}HgS_{sed}$ < $^{201}Hg^{II}$-NOM_{sed} < $^{204}Hg^{II}_{wt}$). On the basis of these results, we conclude that the chemical speciation of Hg^{II} forms, including thermodynamics and kinetics of their solubilization and desorption, is more important for MeHg formation rates in the sediment than are loading rates of nutrient and terrestrial NOM under the experimental conditions applied here. It is worth stressing that the treatment effects on MeHg net formation were minor or nonsignificant despite the relatively large difference in photosynthetic primary production rate between the treatments.

Bioaccumulation of MeHg in the pelagic food web

At the end of the experiment, we collected dominating pelagic (seston size fractions; 50 to 100 μm, 100 to 300 μm, and >300 μm, containing

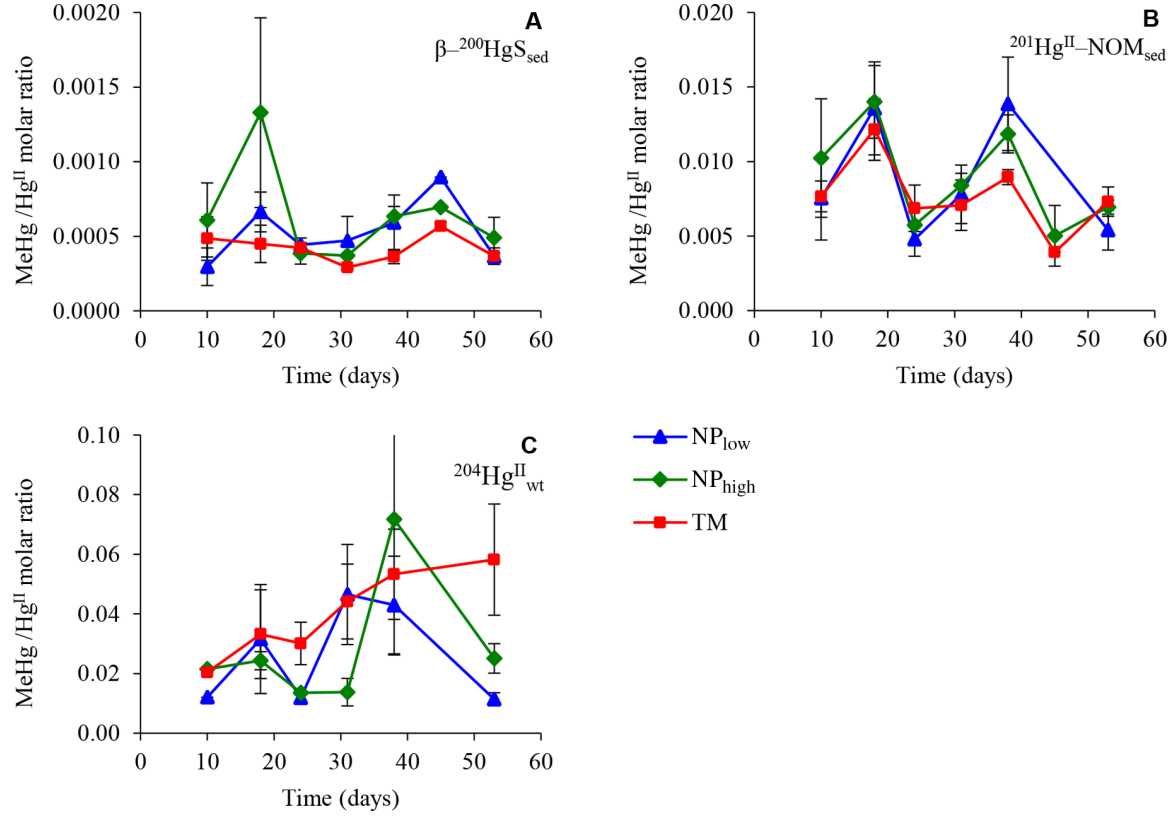

Fig. 1. MeHg net formation in sediment from three different Hg^{II} tracers in response to experimental treatments. The graphs display average MeHg/Hg^{II} molar ratios ± SE ($n = 3$ to 9) determined in mesocosm sediments at different times in response to each of the three experimental treatments: low nutrient input (NP_{low}, blue triangles), high nutrient input (NP_{high}, green diamonds), and terrestrial NOM input (TM, red squares). Each panel displays the net methylation for the specific Hg^{II} isotope tracers added to the mesocosms. (**A**) Metacinnabar added to the sediment (β-$^{200}HgS_{sed}$), (**B**) organic matter Hg complex added to the sediment ($^{201}Hg^{II}$-NOM_{sed}), and (**C**) Hg^{II} added to the water column ($^{204}Hg^{II}_{wt}$). The data for the NP_{low} treatment were reproduced with permission from Jonsson *et al.* (*10*) and the original data sets can be found in fig. S4 of the source paper.

Downloaded from http://advances.sciencemag.org/ on June 27, 2017

zooplankton species) and benthic (*Polychaetes*, *Chironomidae*, Bivalvia, and Amphipoda) biota to determine MeHg bioaccumulation. We observed a considerably higher (range, 3- to 13-fold) MeHg concentration in zooplankton fractions in TM [22 ± 8 pmol g^{-1} dry weight (d.w.) for $Me^{199}Hg_{wt}$] compared to the NP_{low} (3.3 ± 1.2 pmol g^{-1} d.w.) and NP_{high} (5.4 ± 1.3 pmol g^{-1} d.w.) treatments for the $Me^{199}Hg_{wt}$ and $^{204}Hg^{II}{}_{wt}$ tracers added to the water phase (Fig. 2; two-way ANOVA for all size fractions, $P = 0.035$ and $P = 0.049$, respectively). We estimate that the higher concentration of apparently dissolved (0.45-µm filtration) MeHg observed in the TM treatment (fig. S3) could have contributed at most a factor of 2 of increased MeHg content in zooplankton. We attribute the remaining increase (a factor of 2 to 7) in MeHg bioaccumulation for the TM treatment to differences in structure of the pelagic food web as compared to the NP treatments. The MeHg biota accumulation factor (the MeHg concentration in biota divided by the MeHg concentration in water) was significantly increased in the TM [(240 ± 50) × 10^3 for $Me^{199}Hg_{wt}$] compared to the NP_{low} [(70 ± 19) × 10^3] and NP_{high} [(102 ± 2) × 10^3] treatments (two-way ANOVA, $n = 27$, F ratio = 2.74, $P = 0.042$), which shows that the bioaccumulation of MeHg in zooplankton was enhanced in the TM treatment. The bacterially mediated incorporation of carbon in the food web was amplified in TM (72% heterotrophic production compared to 46% for NP_{low} and NP_{high}; Table 1). A calculation (see Materials and Methods) based on the observed photosynthetic and heterotrophic biomass production rates as well as the size class distribution of the phytoplankton community suggested that the number of trophic levels up to zooplankton increased from 2.0 in the NP treatments to 2.3 in the TM treatment. The increased average food web length was further corroborated by an increase (ANOVA, $n = 9$, F ratio = 7.70, $P = 0.022$) in carbon biomass concentration of heterotrophic nanoflagellates (HNFs) by a factor of 6 ($P = 0.018$) and 3 (not significant, $P > 0.05$) in the TM (0.29 ± 0.09 µg C $liter^{-1}$) compared to the NP_{high} (0.047 ± 0.013 µg C $liter^{-1}$) and NP_{low} (0.11 ± 0.03 µg C $liter^{-1}$) treatments, respectively. HNFs are the main predators on bacteria in aquatic systems and thus an important intermediate trophic level. Although the difference in HNF biomass was significant between the TM and NP_{high} treatments, but not between the TM and NP_{low} treatments, the trend is consistent with, and support, the calculated increase in food web length. The on-average longer

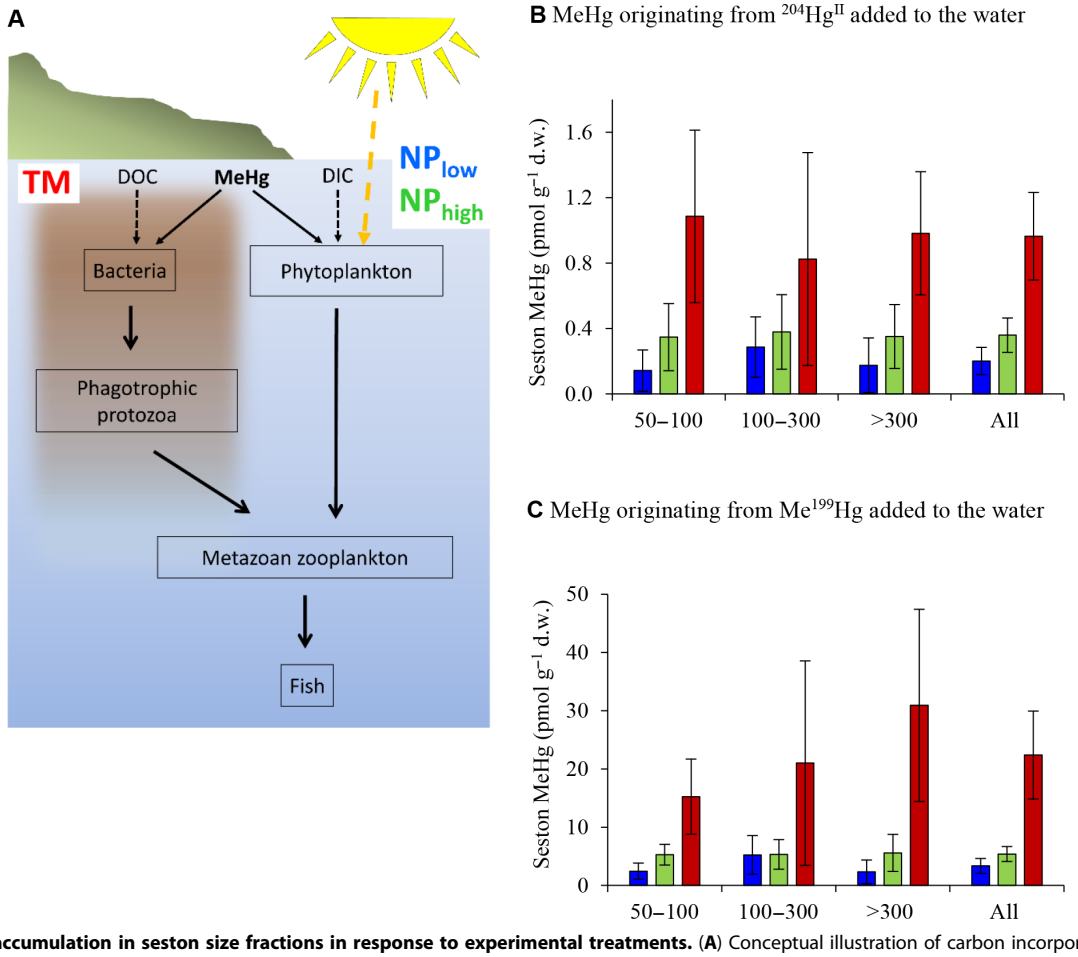

Fig. 2. MeHg bioaccumulation in seston size fractions in response to experimental treatments. (**A**) Conceptual illustration of carbon incorporation and transfer between trophic levels for an autotrophic (NP_{low} and NP_{high})–based and heterotrophic (TM)–based pelagic food web, illustrating an increased number of trophic levels as a potential cause of enhanced MeHg bioaccumulation in a heterotrophic food web. DIC, dissolved inorganic carbon. (**B** and **C**) Average MeHg concentration (pmol g^{-1} d.w.) in seston size fractions (50 to 100, 100 to 300, and >300 µm; $n = 3$ for each fraction) and average for all size fractions ($n = 9$) collected at the end of the experiment (day 57) from the different mesocosm treatments ($n = 3$ per treatment), that is, low nutrient input (NP_{low}, blue bars), high nutrient input (NP_{high}, green bars), and terrestrial NOM input (TM, red bars). Error bars are given as SE. (B) Bioaccumulation of MeHg originating from the Hg^{II} tracer added into the water ($^{204}Hg^{II}{}_{wt}$) and (C) bioaccumulation of MeHg originating from the MeHg tracer added to the water column ($Me^{199}Hg_{wt}$).

Downloaded from http://advances.sciencemag.org/ on June 27, 2017

heterotrophically based food web (*6*, *13*) (Fig. 2A) potentially increases MeHg concentration in zooplankton and higher organisms because MeHg biomagnifies 0.5 to 1.5 log units per trophic level (*32*–*37*). The estimated increase (a factor of 2 to 7) in $Me^{199}Hg$ concentration in zooplankton for TM compared to NP treatment schemes caused by food web structure thus agreed with the theoretically expected enhancement of a factor of 1 to 9 [$(2.3 - 2.0) \times 10^{0.5}$ to $(2.3 - 2.0) \times 10^{1.5}$]. In parallel, the shift to a heterotrophic food web in the TM treatment also resulted in the lowest average total biomass production (see chlorophyll a concentrations in Table 1 and fig. S2), which can contribute to increased MeHg concentration in zooplankton via decreased MeHg biodilution effects (*24*, *37*). Biodilution effects are not well established in estuaries, but on the basis of results from a recent conceptual model, it was proposed that a doubling of algal biomass might decrease MeHg concentration in phytoplankton by ~50% (*24*).

Sorption of humic substances to cell membrane and phytoplankton surfaces has been demonstrated (*38*). The measured C/N molar ratio of the seston size fractions collected from the mesocosms was 5.50 ± 0.27, which agrees well with a previously observed C/N ratio for zooplankton species in the Baltic Sea (*39*, *40*). In contrast, a much higher C/N molar ratio of 25 was measured for the terrestrial organic matter added in the TM treatment. This suggests that the collected seston fractions represented zooplankton samples, free from terrestrial organic matter. On the basis of the C/N molar ratio data, it can thus be concluded that the enhanced MeHg bioaccumulation observed in the TM treatment could not be explained by sorption of dissolved NOM to plankton surfaces.

The observed shift in food web structure and enhanced MeHg bioaccumulation by the TM treatment followed increases in concentrations of DOC (20%) and dissolved humic substances (50%) that can be considered moderate in comparison to natural variability in these variables within and between aquatic ecosystems. Previous studies have reported a maximum (but with high and unexplained variability) MeHg bioaccumulation efficiency in a freshwater alga at ~5 mg $liter^{-1}$ DOC levels (*21*) (investigated range, 1.2 to 38 mg $liter^{-1}$). It has also been demonstrated that MeHg uptake by marine plankton and *Escherichia coli* bacteria was suppressed more by terrestrial DOC compared to marine DOC (investigated range, 0.1 to 100 mg $liter^{-1}$) (*23*). The observed differences in MeHg accumulation in these studies were proposed to be caused by differences in the chemical speciation of MeHg. Because of the relatively small increase (20%) in total DOC and the large fraction (>75%) of terrestrial NOM in the mesocosm water phase, the chemical speciation of MeHg was not affected by the applied treatment schemes in our study (table S2). Our results instead emphasize a shift to a heterotrophic pelagic food web as a major cause behind MeHg biomagnification in pelagic biota in response to moderate, and environmentally realistic, enhanced terrestrial NOM loadings to coastal marine environments. A recent meta-analysis reported that much of the observed among-system variability in MeHg biomagnification in aquatic food webs worldwide remains unexplained (*37*). Given our results, we propose that the relative proportions of autotrophic and heterotrophic production of the food web are important for MeHg biomagnification explanation models.

Predicted impacts on MeHg bioaccumulation from increased discharge following climate scenarios

We applied the experimental data from this study to Hg mass balance calculations (*10*) to analyze the net effect of the experimental manipulations for the processes of MeHg formation and bioaccumulation in coastal ecosystems. Our calculation predicts the concentration of MeHg in zooplankton in the brackish Bothnian Sea (salinity of 5 PSU) coastal areas (here exemplified by the Öre River Estuary; seeMaterials and Methods) to increase as much as a factor of 3 to 6 following the ecological and biogeochemical impacts of a 30% increase (*28*, *29*) in terrestrial runoff (Fig. 3C shows the average predicted increase of a factor of 4.5). In comparison, the calculation predicts only moderate changes in MeHg concentrations in coastal sediment and benthic invertebrates for the different scenarios (Fig. 3, A and B). It should be realized that the predicted three- to sixfold increase of MeHg content in pelagic biota is caused by biogeochemical and ecological changes in the ecosystem and only to a minor extent (15% increase) by increased Hg load.

DISCUSSION

Mesocosm experiments typically have small physical and brief temporal scales in relation to ecosystems, which create intrinsic limitations and uncertainties in upscaling of experimental results (*41*). Regarding MeHg formation and bioaccumulation processes, the specific mesocosm experimental approach used in our study successfully represented relevant natural conditions with respect to four critical circumstances: (i) we used intact sediment cores with a maintained natural redox gradient and a relevant bacterial community structure; (ii) there was a continuous supply of autochthonous organic carbon to the benthic zone; (iii) the nutrient and terrestrial NOM additions created relevant pelagic food webs with respect to both the total biomass production and the proportions of autotrophic and heterotrophic production; (iv) we added Hg isotope tracers with chemical structures relevant for estuarine ecosystems to the mesocosm systems. Because of the realistic approach taken, we propose that the principle findings from our experiment, that is, that terrestrial discharges can mediate trophic shifts and enhance MeHg accumulation in estuarine biota, are also relevant at the ecosystem scale. However, the global scale impact of climate change on MeHg levels in coastal marine food webs is expected to be complex and variable and cannot be predicted with high certainty solely on the basis of an upscaling of the results in our study.

Regarding runoff, the interpretations of data recently compiled by IPCC (*7*) project a highly variable response in runoff, with either increases or decreases, for different regions globally. According to these projections, large regions of the globe may be subjected to a 20 to 30% increase in runoff (climate scenario RCP8.5, fig. S4), as simulated in our study. For northern Eurasia and North America, these increases in runoff are projected to mainly be driven by increased precipitation during winter (*7*) when evapotranspiration is low. Increased terrestrial water runoff to coastal sea areas has already been observed in several regions during the late 20th century (*5*–*7*). Also, a shift from autotrophic to heterotrophic pelagic food web following increased terrestrial NOM discharge, as obtained in our experiment, has been observed not only for experimental systems but also for contrasting natural coastal environments. These environments include tropical (*42*), temperate (*6*, *43*–*46*), and arctic (*47*) regions. However, these trophic shifts have not previously been linked to the biogeochemical cycling of Hg. Our study reveals the importance of incorporating the impact of climate-induced changes in food web structure on MeHg bioaccumulation in future biogeochemical cycling models and risk assessments of Hg.

Downloaded from http://advances.sciencemag.org/ on June 27, 2017

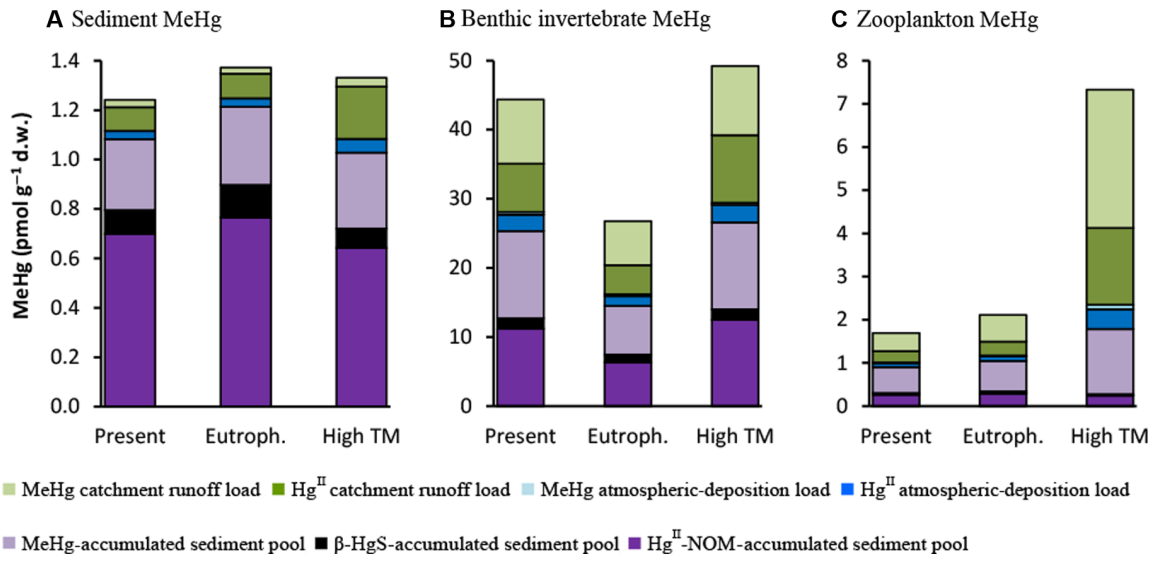

Fig. 3. Modeled MeHg concentrations in sediment and biota for different ecosystem scenarios. Modeled MeHg concentration (table S4) in (**A**) sediment, (**B**) benthic invertebrates, and (**C**) zooplankton. The contributions from individual geochemical Hg^{II} and MeHg pools to the total MeHg concentrations are indicated by different colors. The modeling conditions are relevant to the coastal zone of the northern Bothnian Sea under present conditions (Present), for an eutrophication scenario (Eutroph.), and for an enhanced loading of terrestrial matter (High TM), as projected in climate change scenario Representative Concentration Pathway 8.5 (RCP8.5) for large parts of the world.

MATERIALS AND METHODS

A summary of the experimental setup is given in fig. S1 and table S1. Additional technical details on the mesocosm system, analytical procedures, and the Hg mass balance calculation have been described previously (*10*).

Mesocosm system and preparation

The indoor mesocosm facility is located at the Umeå Marine Sciences Centre at Umeå University and consists of 12 double-mantled high-density polyethylene (HDPE) tubes (5 × 0.74–m diameter) with spatially controlled temperature via a sectioned outer layer of glycol. Sediment and water for the experiment were collected from the Öre River Estuary located in the Bothnian Sea off the Swedish east coast. Nine intact sediment cores (~0.2 × 0.63–m diameter) were manually collected by divers (coordinates: 63°33.905′N, 19°50.898′E) at a water depth of 5 to 7 m using custom-made HDPE (same material as the mesocosm systems) sampling device cylinders with a detachable bottom and a detachable lid. The cylinders were immersed in undisturbed sediment, and the bottom plate was inserted through a notch in the cylinder wall. The lid was placed on a second notch a few centimeters above the sediment surface. The cores were stored for up to 7 days in the dark, at 15°C in seawater-filled barrels. Brackish water (salinity of 5 PSU) was collected through a 0.3-mm sieve at water depths of 2 and 8 m with inlets located 800 m from land via a pumping system. All mesocosms were filled in parallel to assure a similar distribution of, for example, planktonic organism communities. We used three replicate mesocosms with sediment and water and one mesocosm with only water for each of the three treatments. Metal halogen lamps (150 W) (MASTERColour CDM-T 150W/942 G12 1CT) were used as light sources with a light/dark cycle of 12:12 hours. The daily cumulative photosynthetically active radiation light flux corresponded to typical conditions in the photic zone during summer in the Bothnian Sea (*48*). The temperature of the water column was controlled in three sections with 14°C in the top layer and 16°C in the middle layer, which induced mixing by thermal convection in the upper part (completely mixed within a few hours of this part) and a thermocline at ~3.2 m. The lowest section was kept at 10°C. The mesocosm water temperature was close to 15°C from the surface to a 3.0-m depth and decreased linearly to 9°C from 3.0 to 4.7 m.

Nitrate, ammonium, and phosphate were added according to the scheme in table S5. Terrestrial NOM was extracted (Amberlite IRC-748I iminodiacetic acid chelating cation exchange resin, followed by sequential filtration through 90- to 100- and 0.45-μm filters) from soil collected at the Nyänget catchment, located at Svartberget in northern Sweden (64°14′N, 19°46′E) (*49*). Soil was sampled at the stream bank of the "Västrabäcken" just above the water surface of the stream. Soil from this location has previously been characterized with respect to Hg and organic sulfur speciation (*50*). The final terrestrial NOM extract added to TM mesocosms contained DOC (800 ± 90 mg liter^{-1}), humic substances (1.95 ± 0.09 mg liter^{-1}) (quinine sulfate units), <0.05 μM NO_3^-, 32 ± 7 μM NO_2^-, 65 ± 14 μM NH_4^+, 1900 ± 180 μM total N, 10 ± 1 μM PO_4^{3-}, 110 ± 19 μM total P, and 130 ± 17 μM Si. The terrestrial NOM extract was added to TM mesocosms on days 1 (5 liters per tank), 9 (2.5 liters), 19 (2.5 liters), and 37 (2.5 liters), resulting in added DOC concentrations of 2, 1, 1, and 1 mg of DOC liter^{-1}, respectively, in the 2000-liter mesocosm tanks. The date for the first nutrient and terrestrial NOM additions was referred to as day 1, and the experiment was then continued for 58 days.

Hg isotope tracer preparation and additions

Hg^{II} enriched in ^{196}Hg (50%), ^{198}Hg (92.78%), ^{199}Hg (91.95%), ^{200}Hg (96.41%), ^{201}Hg (98.11%), or ^{204}Hg (98.11%) (as HgO or $HgCl_2$) was purchased from Oak Ridge National Laboratory (TN, USA). Isotopically enriched β-^{200}HgS(s), $^{201}Hg^{II}$-NOM, $Me^{198}Hg$-NOM tracers, and MeHg(aq) were synthesized according to previously established procedures (*26*). A slurry mixture of β-^{200}HgS(s), $^{201}Hg^{II}$-NOM, and $Me^{198}Hg$-NOM was prepared within 1 hour before it was injected into the intact sediment cores using an electronic 12-channel pipette. Amounts of 12 × 100 μl of the slurry was injected ~0.5 cm below the sediment surface in 10-μl

Downloaded from http://advances.sciencemag.org/ on June 27, 2017

portions with a 1-cm *x*-axis distance and a 0.8-cm *y* axis distance (given by the distance between pipette tips), resulting in 1.13 injections per cm^2. In total, 3264 injections were made per sediment core, covering ~92% of the sediment surface. Sediment cores were then immersed into the water-filled mesocosm (with the lid removed after placement of the sediment cylinders). The $^{204}Hg^{II}_{wt}$ and $Me^{199}Hg_{wt}$ tracers were added day 2 of the experiment to the upper part of the water column (above the thermocline) 20 min after the light was turned off. The total added amount of the $^{204}Hg^{II}_{wt}$ and $Me^{199}Hg_{wt}$ tracers were 46 and 4.6 nmol, corresponding to a concentration of 24 and 2.4 pmol $liter^{-1}$, respectively, in the mesocosm water. For β-$^{200}HgS_{sed}$, $^{201}Hg^{II}$-NOM_{sed}, and $Me^{198}Hg$-NOM_{sed}, 1300, 130, and 9.0 nmol were added, corresponding to concentrations of 1040, 104, and 7.3 pmol g^{-1} d.w., respectively, in the sediment. The solid/adsorbed-phase Hg tracers were synthesized and added to the sediment as defined thermodynamically favored chemical forms, that is, β-HgS(s) and Hg bond to thiol groups in NOM, $Hg(SR\text{-}NOM)_2$, and MeHgSR-NOM, respectively. The dissolved tracers were added to the water phase as labile complexes dominated by $Hg(OH)_2^0$ and $MeHgOH^0$, respectively. Thermodynamic calculations showed that chemical speciation of Hg also in the aqueous phase of the mesocosms for all treatments were completely dominated by $Hg(SR\text{-}NOM)_2$ and MeHgSR-NOM complexes (table S2). The dissolved Hg tracers are expected to reach equilibrium with components in the aqueous phase within a relatively short time (hours to maximum a few days) (*51*, *52*) compared to the slower rate (days to weeks) (*53*–*55*) to form β-HgS(s) and adsorbed phases of $Hg(SR\text{-}NOM)_2$ in the sediment. In contrast, the solid/adsorbed-phase Hg tracers used in our study needed to be synthesized to thermodynamically favored chemical forms before addition to the sediment. The Hg tracers added to the water phase were thus used as proxies for both terrestrial and atmospheric Hg inputs, and the tracers added to the sediment were taken to represent sources for in situ MeHg formation.

Sampling procedures

Water and sediment were sampled once a week from the mesocosms for biological and chemical analyses. Water was sampled from defined depths using a 50-ml plastic syringe and plastic tubing into 15- or 50-ml Falcon tubes for determination of biological and ancillary chemical parameters. For MeHg and total Hg measurements, water was separately sampled using Teflon tubing and a peristaltic pump with online filtration (0.45-μm Millex) in acid-washed PE bottles (0.5 or 1 l). Sediment subcores (10 to 15 × 4.2–cm diameter) were sampled from the mesocosm sediments during the experiment using a custom-made sampler with 12 fixed sampling positions designed for the mesocosms (*10*).

Seston size fractions were collected at the end of the experiment from the entire water column above a 0.77-m height through 300-, 90 to 100-, and 50-μm plankton nets in series. The seston fractions were washed with filtrated (0.45-μm) mesocosm water and freeze-dried. Benthic invertebrates were collected manually through a sediment sieve, left in filtrated mesocosm water overnight, and then freeze-dried. Sedimented material was collected in cylinder traps immersed in mesocosms without [n = 4 $mesocosm^{-1}$; inner diameter (i.d.), 0.106 m] and with sediment (n = 1 $mesocosm^{-1}$; i.d., 0.085 m).

Chemical and biological analyses

All chemical and biological analysis protocols used have previously been described in detail (*10*) and are summarized in Supplementary Materials and Methods.

Pelagic food web structure modeling

The pelagic food web consisted of phytoplankton (primary producers), heterotrophic bacteria, protozoa, and mesozooplankton (dominated by the copepod *Eurytemora affinis*). The food web was modeled from measured photosynthetic primary and heterotrophic bacterial biomass production and the size class distribution of the phytoplankton community. A well-established structure of the pelagic food web in the study area (*6*, *56*) was used in which bacteria were grazed by flagellates, which were grazed by ciliates, which in turn were predated by mesozooplankton. Phytoplankton were grazed by flagellates, ciliates, or mesozooplankton depending on their size. A trophic transfer efficiency (TTE) of 30% was assumed (*56*, *57*). Food web efficiency (FWE) was calculated as the production by the highest trophic level (mesozooplankton) divided by the production by the lowest trophic level (primary + bacterial production) (*56*). The number of trophic levels was calculated as follows: number of trophic levels = 1 + log(FWE)/log(TTE).

Statistics

In the mesocosm experiment, each replicate was resampled at regular intervals, and repeated-measures ANOVA was used to test for differences between treatments over time. If conditions for compound symmetry using Mauchly's test for sphericity (*58*) were not met, Greenhouse-Geisser ε (*59*) and Huynh-Feldt ε (*60*) were used for correction of the *F* test. Differences in MeHg concentrations in biota were tested by two-way ANOVA using mesocosm treatments and size fractions of plankton (50 to 100, 100 to 300, and >300 μm) as independent variables. To test for differences between treatments, Tukey's test was used for MeHg concentrations, and Student's *t* test was used for MeHg bioaccumulation. Differences in HNF biomass in the mesocosms were tested by ANOVA, followed by Tukey's test for pairwise comparison of biomasses between treatments. The null-hypothesis was verified by $\alpha \geq 0.05$ (no difference among treatments) unless otherwise stated. All statistical calculations were done using JMP (version 10.0.0, SAS Institute Inc.) software.

SUPPLEMENTARY MATERIALS

Supplementary material for this article is available at http://advances.sciencemag.org/cgi/content/full/3/1/e1601239/DC1

Supplementary Materials and Methods

eq. S1. Calculation of MeHg concentration (pmol g^{-1} d.w.) in sediment.

eq. S2. Calculation of MeHg concentration (pmol g^{-1} d.w.) in biota.

fig. S1. Schematic illustration of the mesocosm experiment setup.

fig. S2. Pelagic biological productivity parameters.

fig. S3. Total ^{204}Hg and $Me^{199}Hg$ concentrations in water.

fig. S4. Projected changes in runoff following climate scenario RCP8.5 (IPCC) (*7*).

fig. S5. Sedimentation rate of NOM.

table S1. Schematic description of the mesocosm experiment treatments.

table S2. Chemical speciation calculations for Hg^{II} and MeHg in the mesocosm water phase.

table S3. Statistics for the treatment effects from repeated-measures ANOVA for eight response variables (Table 1) in mesocosm.

table S4. Input data for the Hg mass balance calculations based on eqs. S1 and S2.

table S5. Nutrient addition scheme for the mesocosm water phase.

References (*61*, *62*)

REFERENCES AND NOTES

1. J. Munthe, R. A. Bodaly, B. A. Branfireun, C. T. Driscoll, C. C. Gilmour, R. Harris, M. Horvat, M. Lucotte, O. Malm, Recovery of mercury-contaminated fisheries. *Ambio* **36**, 33–44 (2007).
2. D. P. Krabbenhoft, E. M. Sunderland, Global change and mercury. *Science* **341**, 1457–1458 (2013).

Downloaded from http://advances.sciencemag.org/ on June 27, 2017

3. G. A. Stern, R. W. Macdonald, P. M. Outridge, S. Wilson, J. Chételat, A. Cole, H. Hintelmann, L. L. Loseto, A. Steffen, F. Wang, C. Zdanowicz, How does climate change influence arctic mercury? *Sci. Total Environ.* **414**, 22–42 (2012).
4. R. Costanza, R. d'Arge, R. de Groot, S. Farber, M. Grasso, B. Hannon, K. Limburg, S. Naeem, R. V. O'Neill, J. Paruelo, R. G. Raskin, P. Sutton, M. van den Belt, The value of the world's ecosystem services and natural capital. *Nature* **387**, 253–260 (1997).
5. B. J. Peterson, R. M. Holmes, J. W. McClelland, C. J. Vörösmarty, R. B. Lammers, A. I. Shiklomanov, I. A. Shiklomanov, S. Rahmstorf, Increasing river discharge to the Arctic Ocean. *Science* **298**, 2171–2173 (2002).
6. J. Wikner, A. Andersson, Increased freshwater discharge shifts the trophic balance in the coastal zone of the northern Baltic Sea. *Glob. Chang. Biol.* **18**, 2509–2519 (2012).
7. Intergovernmental Panel on Climate Change, *Climate Change 2013: The Physical Science Basis* (Cambridge Univ. Press, 2013).
8. J. E. Bauer, W.-J. Cai, P. A. Raymond, T. S. Bianchi, C. S. Hopkinson, P. A. G. Regnier, The changing carbon cycle of the coastal ocean. *Nature* **504**, 61–70 (2013).
9. W. F. Fitzgerald, C. H. Lamborg, C. R. Hammerschmidt, Marine biogeochemical cycling of mercury. *Chem. Rev.* **107**, 641–662 (2007).
10. S. Jonsson, U. Skyllberg, M. B. Nilsson, E. Lundberg, A. Andersson, E. Björn, Differentiated availability of geochemical mercury pools controls methylmercury levels in estuarine sediment and biota. *Nat. Commun.* **5**, 4624 (2014).
11. J. A. Fisher, D. J. Jacob, A. L. Soerensen, H. M. Amos, A. Steffen, E. M. Sunderland, Riverine source of Arctic Ocean mercury inferred from atmospheric observations. *Nat. Geosci.* **5**, 499–504 (2012).
12. A. T. Schartup, P. H. Balcom, A. L. Soerensen, K. Gosnell, R. Calder, R. P. Mason, E. M. Sunderland, Freshwater discharges drive high levels of methylmercury in Arctic marine biota. *Proc. Natl. Acad. Sci. U.S.A.* **112**, 11789–11794 (2015).
13. J. Sandberg, A. Andersson, S. Johansson, J. Wikner, Pelagic food web structure and carbon budget in the northern Baltic Sea: Potential importance of terrigenous carbon. *Mar. Ecol. Prog. Ser.* **268**, 13–29 (2004).
14. T. J. Smayda, The suspension and sinking of phytoplankton in the sea. *Oceanogr. Mar. Biol. Ann. Rev.* **8**, 353–414 (1970).
15. S. B. Baines, M. L. Pace, The production of dissolved organic matter by phytoplankton and its importance to bacteria: Patterns across marine and freshwater systems. *Limnol. Oceanogr.* **36**, 1078–1090 (1991).
16. E. S. Kritzberg, J. J. Cole, M. L. Pace, W. Graneli, D. L. Bade, Autochthonous versus allochthonous carbon sources of bacteria: Results from whole-lake C-13 addition experiments. *Limnol. Oceanogr.* **49**, 588–596 (2004).
17. A. Drott, L. Lambertsson, E. Bjorn, U. Skyllberg, Importance of dissolved neutral mercury sulfides for methyl mercury production in contaminated sediments. *Environ. Sci. Technol.* **41**, 2270–2276 (2007).
18. M. Kim, S. Han, J. Gieskes, D. D. Deheyn, Importance of organic matter lability for monomethylmercury production in sulfate-rich marine sediments. *Sci. Total Environ.* **409**, 778–784 (2011).
19. G. C. Compeau, R. Bartha, Sulfate-reducing bacteria: Principal methylators of mercury in anoxic estuarine sediment. *Appl. Environ. Microbiol.* **50**, 498–502 (1985).
20. J. M. Parks, A. Johs, M. Podar, R. Bridou, R. A. Hurt Jr., S. D. Smith, S. J. Tomanicek, Y. Qian, S. D. Brown, C. C. Brandt, A. V. Palumbo, J. C. Smith, J. D. Wall, D. A. Elias, L. Liang, The genetic basis for bacterial mercury methylation. *Science* **339**, 1332–1335 (2013).
21. P. R. Gorski, D. E. Armstrong, J. P. Hurley, D. P. Krabbenhoft, Influence of natural dissolved organic carbon on the bioavailability of mercury to a freshwater alga. *Environ. Pollut.* **154**, 116–123 (2008).
22. A. C. Luengen, N. S. Fisher, B. A. Bergamaschi, Dissolved organic matter reduces algal accumulation of methylmercury. *Environ. Toxicol. Chem.* **31**, 1712–1719 (2012).
23. A. T. Schartup, U. Ndu, P. H. Balcom, R. P. Mason, E. M. Sunderland, Contrasting effects of marine and terrestrially derived dissolved organic matter on mercury speciation and bioavailability in seawater. *Environ. Sci. Technol.* **49**, 5965–5972 (2015).
24. C. T. Driscoll, C. Y. Chen, C. R. Hammerschmidt, R. P. Mason, C. C. Gilmour, E. M. Sunderland, B. K. Greenfield, K. L. Buckman, C. H. Lamborg, Nutrient supply and mercury dynamics in marine ecosystems: A conceptual model. *Environ. Res.* **119**, 118–131 (2012).
25. N. Gantner, M. Power, D. Iqaluk, M. Meili, H. Borg, M. Sundbom, K. R. Solomon, G. Lawson, D. C. Muir, Mercury concentrations in landlocked Arctic Char (*Salvelinus alpinus*) from the Canadian Arctic. Part I: Insights from trophic relationships in 18 lakes. *Environ. Toxicol. Chem.* **29**, 621–632 (2010).
26. S. Jonsson, U. Skyllberg, M. B. Nilsson, P.-O. Westlund, A. Shchukarev, E. Lundberg, E. Björn, Mercury methylation rates for geochemically relevant Hg^{II} species in sediments. *Environ. Sci. Technol.* **46**, 11653–11659 (2012).
27. A. Andersson, S. Hajdu, P. Haecky, J. Kuparinen, J. Wikner, Succession and growth limitation of phytoplankton in the Gulf of Bothnia (Baltic Sea). *Mar. Biol.* **126**, 791–801 (1996).
28. A. Omstedt, M. Edman, B. Claremar, P. Frodin, E. Gustafsson, C. Humborg, H. Hägg, M. Mörth, A. Rutgersson, G. Schurges, B. Smith, T. Wällstedt, A. Yurova, Future changes in the Baltic Sea acid–base (pH) and oxygen balances. *Tellus Ser. B Chem. Phys. Meteorol.* **64**, 19586 (2012).
29. HELCOM, *Climate Change in the Baltic Sea Area, Baltic Sea Environment Proceedings No. 137* (Erweko Oy, Finland, 2013).
30. V. Alling, C. Humborg, C. M. Morth, L. Rahm, F. Pollehne, Tracing terrestrial organic matter by delta(34)S and delta(13)C signatures in a subarctic estuary. *Limnol. Oceanogr.* **53**, 2594–2602 (2008).
31. T. Zhang, K. H. Kucharzyk, B. Kim, M. A. Deshusses, H. Hsu-Kim, Net methylation of mercury in estuarine sediment microcosms amended with dissolved, nanoparticulate, and microparticulate mercuric sulfides. *Environ. Sci. Technol.* **48**, 9133–9141 (2014).
32. W. R. Hill, A. J. Stewart, G. E. Napolitano, Mercury speciation and bioaccumulation in lotic primary producers and primary consumers. *Can. J. Fish. Aquat. Sci.* **53**, 812–819 (1996).
33. C. J. Watras, R. C. Back, S. Halvorsen, R. J. M. Hudson, K. A. Morrison, S. P. Wente, Bioaccumulation of mercury in pelagic freshwater food webs. *Sci. Total Environ.* **219**, 183–208 (1998).
34. A. R. Stewart, M. K. Saiki, J. S. Kuwabara, C. N. Alpers, M. Marvin-DiPasquale, D. P. Krabbenhoft, Influence of plankton mercury dynamics and trophic pathways on mercury concentrations of top predator fish of a mining-impacted reservoir. *Can. J. Fish. Aquat. Sci.* **65**, 2351–2366 (2008).
35. K. R. Rolfhus, B. D. Hall, B. A. Monson, M. J. Paterson, J. D. Jeremiason, Assessment of mercury bioaccumulation within the pelagic food web of lakes in the western Great Lakes region. *Ecotoxicology* **20**, 1520–1529 (2011).
36. T. D. Jardine, K. A. Kidd, N. O'Driscoll, Food web analysis reveals effects of pH on mercury bioaccumulation at multiple trophic levels in streams. *Aquat. Toxicol.* **132**, 46–52 (2013).
37. R. A. Lavoie, T. D. Jardine, M. M. Chumchal, K. A. Kidd, L. M. Campbell, Biomagnification of mercury in aquatic food webs: A worldwide meta-analysis. *Environ. Sci. Technol.* **47**, 13385–13394 (2013).
38. P. G. C. Campbell, M. R. Twiss, K. J. Wilkinson, Accumulation of natural organic matter on the surfaces of living cells: Implications for the interaction of toxic solutes with aquatic biota. *Can. J. Fish. Aquat. Sci.* **54**, 2543–2554 (1997).
39. M. Koski, Carbon: Nitrogen ratios of Baltic Sea copepods—Indication of mineral limitation? *J. Plankton Res.* **21**, 1565–1573 (1999).
40. J. Walve, U. Larsson, Carbon, nitrogen and phosphorus stoichiometry of crustacean zooplankton in the Baltic Sea: Implications for nutrient recycling. *J. Plankton Res.* **21**, 2309–2321 (1999).
41. J. E. Petersen, J. C. Cornwell, W. M. Kemp, Implicit scaling in the design of experimental aquatic ecosystems. *Oikos* **85**, 3–18 (1999).
42. J. J. Barrera-Alba, S. M. F. Gianesella, G. A. O. Moser, F. M. Saldanha-Corrêa, Influence of allochthonous organic matter on bacterioplankton biomass and activity in a eutrophic, sub-tropical estuary. *Estuar. Coast. Shelf Sci.* **82**, 84–94 (2009).
43. R. W. Howarth, D. P. Swaney, T. J. Butler, R. Marino, Climatic control on eutrophication of the Hudson River estuary. *Ecosystems* **3**, 210–215 (2000).
44. N. F. Caraco, J. J. Cole, in *Hudson River Fishes and their Environment,* J. R. Waldman, K. E. Limburg, D. L. Strayer, Eds. (American Fisheries Society, Bethesda, 2006), vol. 51, pp. 63–74.
45. J. Karlsson, P. Byström, J. Ask, P. Ask, L. Persson, M. Jansson, Light limitation of nutrient-poor lake ecosystems. *Nature* **460**, 506–509 (2009).
46. J. N. Hitchcock, S. M. Mitrovic, T. Kobayashi, D. P. Westhorpe, Responses of estuarine bacterioplankton, phytoplankton and zooplankton to dissolved organic carbon (DOC) and inorganic nutrient additions. *Estuar. Coasts* **33**, 78–91 (2010).
47. T. F. Thingstad, R. G. J. Bellerby, G. Bratbak, K. Y. Børsheim, J. K. Egge, M. Heldal, A. Larsen, C. Neill, J. Nejstgaard, S. Norland, R.-A. Sandaa, E. F. Skjoldal, T. Tanaka, R. Thyrhaug, B. Töpper, Counterintuitive carbon-to-nutrient coupling in an Arctic pelagic ecosystem. *Nature* **455**, 387–390 (2008).
48. A. Andersson, P. Haecky, Å. Hagström, Effect of temperature and light on the growth of micro-plankton nano-plankton and pico-plankton - impact on algal succession. *Mar. Biol.* **120**, 511–520 (1994).
49. K. Bishop, Y.-H. Lee, C. Pettersson, B. Allard, Terrestrial sources of methylmercury in surface waters: The importance of the riparian zone on the Svartberget catchment. *Water Air Soil Pollut.* **80**, 435–444 (1995).
50. U. Skyllberg, J. Qian, W. Frech, K. Xia, W. F. Bleam, Distribution of mercury, methyl mercury and organic sulphur species in soil, soil solution and stream of a boreal forest catchment. *Biogeochemistry* **64**, 53–76 (2003).

Downloaded from http://advances.sciencemag.org/ on June 27, 2017

51. H. Hintelmann, R. Harris, Application of multiple stable mercury isotopes to determine the adsorption and desorption dynamics of Hg(II) and MeHg to sediments. *Mar. Chem.* **90**, 165–173 (2004).
52. C. L. Miller, G. Southworth, S. Brooks, L. Y. Liang, B. H. Gu, Kinetic controls on the complexation between mercury and dissolved organic matter in a contaminated environment. *Environ. Sci. Technol.* **43**, 8548–8553 (2009).
53. U. Skyllberg, K. Xia, P. R. Bloom, E. A. Nater, W. F. Bleam, Binding of mercury(II) to reduced sulfur in soil organic matter along upland-peat soil transects. *J. Environ. Qual.* **29**, 855–865 (2000).
54. A. J. Slowey, Rate of formation and dissolution of mercury sulfide nanoparticles: The dual role of natural organic matter. *Geochim. Cosmochim. Acta* **74**, 4693–4708 (2010).
55. L. Liao, H. M. Selim, R. D. DeLaune, Mercury adsorption-desorption and transport in soils. *J. Environ. Qual.* **38**, 1608–1616 (2009).
56. J. Berglund, U. Müren, U. Båmstedt, A. Andersson, Efficiency of a phytoplankton-based and a bacteria-based food web in a pelagic marine system. *Limnol. Oceanogr.* **52**, 121–131 (2007).
57. D. Straile, Gross growth efficiencies of protozoan and metazoan zooplankton and their dependence on food concentration, predator-prey weight ratio, and taxonomic group. *Limnol. Oceanogr.* **42**, 1375–1385 (1997).
58. J. W. Mauchly, Significance test for sphericity of a normal *n* -variate distribution. *Ann. Math. Statist.* **11**, 204–209 (1940).
59. S. W. Greenhouse, S. Geisser, On methods in the analysis of profile data. *Psychometrika* **24**, 95–112 (1959).
60. H. Huynh, L. S. Feldt, Estimation of the box correction for degrees of freedom from sample data in randomized block and split-plot designs. *J. Educ. Stat.* **1**, 69–82 (1976).
61. P. G. Coble, S. A. Green, N. V. Blough, R. B. Gagosian, Characterization of dissolved organic-matter in the Black-Sea by fluorescence spectroscopy. *Nature* **348**, 432–435 (1990).
62. U. Skyllberg, Competition among thiols and inorganic sulfides and polysulfides for Hg and MeHg in wetland soils and sediments under suboxic conditions: Illumination of controversies and implications for MeHg net production. *J. Geophys. Res.* **113**, G00C03 (2008).

Acknowledgments

Funding: This work was supported by the Swedish Research Council (grant 2008-4363); the Kempe Foundation (grants SMK-2942, SMK-2745, and JCK-2413); Umeå Marine Sciences Centre, Umeå University (including a Young Researcher Award to E.B.); and the Knut and Alice Wallenberg Foundation (grant 94.160). Financial support to A.A. was received from the Strategic Marine Environmental Research program Ecosystem dynamics in the Baltic Sea in a changing climate perspective (EcoChange). The use of laboratory facilities as well as assistance from the staff at the Umeå Marine Sciences Centre is gratefully acknowledged. A. M. Nguyen and H. Genberg are gratefully acknowledged for assistance with the experimental work. **Author contributions:** S.J., A.A., M.B.N., U.S., E.L., and E.B. designed the study. S.J. and E.B. carried out the experimental work and data analysis. A.A., M.B.N., U.S., E.L., J.K.S., and S.Å. contributed with data analysis. S.J., A.A., M.B.N., J.K.S., U.S., and E.B. wrote the paper, and all authors edited and revised the paper. **Competing interests:** The authors declare that they have no competing interests. **Data and materials availability:** All data needed to evaluate the conclusions in the paper are present in the paper and/or the Supplementary Materials. Additional data related to this paper may be requested from the authors.

Submitted 1 June 2016
Accepted 27 November 2016
Published 27 January 2017
10.1126/sciadv.1601239

Citation: S. Jonsson, A. Andersson, M. B. Nilsson, U. Skyllberg, E. Lundberg, J. K. Schaefer, S. Åkerblom, E. Björn, Terrestrial discharges mediate trophic shifts and enhance methylmercury accumulation in estuarine biota. *Sci. Adv.* **3**, e1601239 (2017).

Downloaded from http://advances.sciencemag.org/ on June 27, 2017

ScienceAdvances

Terrestrial discharges mediate trophic shifts and enhance methylmercury accumulation in estuarine biota

Sofi Jonsson, Agneta Andersson, Mats B. Nilsson, Ulf Skyllberg, Erik Lundberg, Jeffra K. Schaefer, Staffan Åkerblom and Erik Björn

Sci Adv **3** (1), e1601239.
DOI: 10.1126/sciadv.1601239

ARTICLE TOOLS http://advances.sciencemag.org/content/3/1/e1601239

SUPPLEMENTARY MATERIALS http://advances.sciencemag.org/content/suppl/2017/01/23/3.1.e1601239.DC1

REFERENCES This article cites 59 articles, 7 of which you can access for free
http://advances.sciencemag.org/content/3/1/e1601239#BIBL

PERMISSIONS http://www.sciencemag.org/help/reprints-and-permissions

Use of this article is subject to the Terms of Service

Science Advances (ISSN 2375-2548) is published by the American Association for the Advancement of Science, 1200 New York Avenue NW, Washington, DC 20005. 2017 © The Authors, some rights reserved; exclusive licensee American Association for the Advancement of Science. No claim to original U.S. Government Works. The title *Science Advances* is a registered trademark of AAAS.

Downloaded from http://advances.sciencemag.org/ on June 27, 2017